

DETC2009-86868

ON MEASURES OF COUPLING BETWEEN THE ARTIFACT AND CONTROLLER OPTIMAL DESIGN PROBLEMS

Diane L. Peters*

Panos Y. Papalambros

A. Galip Ulsoy

Department of Mechanical Engineering

University of Michigan

Ann Arbor, Michigan 48109

Email: dlpeters@umich.edu, pyp@umich.edu, ulsoy@umich.edu

ABSTRACT

Optimization of smart products requires optimizing both the artifact design and its controller. The presence of coupling between the design and control problems is an important consideration in choosing the system optimization method. Several measures of coupling have been proposed based on different viewpoints of the system. In this paper, two measures of coupling, a vector based on optimality conditions and a matrix derived from an extension of the global sensitivity equations, are shown to be related under certain conditions and be consistent in their coupling determination. The measures' physical interpretation and relative ease of use are discussed using the example of a positioning gantry. A further relation is derived between one measure and a modified sequential formulation that would give sufficiently close results to the true solutions.

NOMENCLATURE

\mathbf{d}_a Vector of artifact design variables
 \mathbf{d}_c Vector of controller design variables
 f_a Artifact objective function
 f_c Controller objective function
 F System objective function
 w_a Weight assigned to artifact objective
 w_c Weight assigned to controller objective

Γ_v Uni-directional coupling vector derived from optimality conditions
 Γ_{vb} Bi-directional coupling vector derived from optimality conditions
 Γ_m Coupling matrix based on Global Sensitivity Equations
 f_i Objective function for sub-system i in coupling matrix
 \mathbf{x}_i Design variables associated with subsystem i in coupling matrix
 \mathbf{y}_{ij} Interaction variables between subsystems i and j in coupling matrix
 $\hat{\mathbf{y}}_{ij}$ Local copy of interaction variables \mathbf{y}_{ij}
 $\hat{\mathbf{x}}_i$ Local copy of the variables \mathbf{x}_i
 N Number of subsystems present in coupling matrix
 \mathbf{x} States of the example system
 Z Displacement of the mass in the example system
 \mathbf{C} Vector determining example system output from system states
 \mathbf{A} State matrix determining the unforced response of the example system
 \mathbf{B} Vector determining the forced response of the example system
 m Generalized mass term in differential equation describing example system
 b Generalized damping term in differential equation describing example system

*Address all correspondence to this author.

- k Generalized stiffness term in differential equation describing example system
- u Control input to example system
- V Voltage applied to example system
- M Mass in example system
- r Radius of pulley in example system
- R_a Armature resistance in example system
- k_t Torque constant of motor in example system
- k_s Spring constant of spring in example system

1 INTRODUCTION

In the optimal design and control of systems, there are typically two objectives present. There is an objective function f_a for the physical system, or artifact, and another objective f_c for the controller applied to the system. The full set of variables in this problem consists of artifact design variables \mathbf{d}_a and controller design variables \mathbf{d}_c . The optimization problem for the system is typically formulated as a combination of the individual objectives. Often, this objective is a linear combination, with weights applied to the individual objectives, as follows.

$$\min_{\mathbf{d}_a, \mathbf{d}_c} w_a f_a + w_c f_c \quad (1)$$

subject to

$$\mathbf{g}(\mathbf{d}_a, \mathbf{d}_c) \leq \mathbf{0} \quad (2)$$

$$\mathbf{h}(\mathbf{d}_a, \mathbf{d}_c) = \mathbf{0} \quad (3)$$

Coupling can be either uni-directional or bi-directional. In uni-directional coupling, the artifact objective function and constraints are functions only of the artifact variables, while the controller objective function and constraints depend on both artifact and controller variables, i.e., $f_a = f_a(\mathbf{d}_a)$, $\mathbf{g}_a = \mathbf{g}_a(\mathbf{d}_a)$, $\mathbf{h}_a = \mathbf{h}_a(\mathbf{d}_a)$, $f_c = f_c(\mathbf{d}_a, \mathbf{d}_c)$, $\mathbf{g}_c = \mathbf{g}_c(\mathbf{d}_a, \mathbf{d}_c)$, and $\mathbf{h}_c = \mathbf{h}_c(\mathbf{d}_a, \mathbf{d}_c)$. In bi-directional coupling, the artifact objective function and constraints as well as the controller objective function and constraints depend on both sets of design variables, i.e. $f_a = f_a(\mathbf{d}_a, \mathbf{d}_c)$, $\mathbf{g}_a = \mathbf{g}_a(\mathbf{d}_a, \mathbf{d}_c)$, $\mathbf{h}_a = \mathbf{h}_a(\mathbf{d}_a, \mathbf{d}_c)$, $f_c = f_c(\mathbf{d}_a, \mathbf{d}_c)$, $\mathbf{g}_c = \mathbf{g}_c(\mathbf{d}_a, \mathbf{d}_c)$, and $\mathbf{h}_c = \mathbf{h}_c(\mathbf{d}_a, \mathbf{d}_c)$. There are many systems which exhibit coupling between the artifact and controller design, including structures [1–3], robotic arms and planar mechanisms [4–6], and micro-electrical mechanical systems [7–9].

There are a number of issues involved in the solution of coupled problems, including quantifying the strength of the coupling. This paper compares two measures of coupling previously proposed, one based on optimality conditions and another derived from global sensitivity equations, and shows that they are equivalent for certain problems. Section 2 of this paper presents

an explanation of the two coupling measures and their range of applicability. In Section 3, conditions are set out for a certain problem formulation, and the equivalence of the coupling measures is demonstrated for that problem formulation. Section 4 discusses the relation between the coupling vector and the slope of the Pareto frontier. Section 5 uses an example to illustrate the relation derived between the two measures. Section 6 relates the coupling vector to the accuracy of a surrogate function for ease of control, and Section 7 extends the coupling vector to the case of bi-directional coupling. This is followed by concluding remarks in Section 8.

2 DEFINITION OF COUPLING MEASURES

In previous work by Reyer et al. [10, 11], the concept of coupling in “co-design”, or combined optimal design of an artifact and its controller, was introduced. These concepts were demonstrated in the optimal design of an electric DC motor and its controller [10, 11]. The existence of coupling was determined by the existence of interaction variables, but was not quantified to determine its strength. Bi-directional coupling was considered in this work.

In later work by Fathy et al. [12, 13], only uni-directional coupling was considered, and it was assumed that the system objective function was a weighted sum of the two individual objectives, i.e. $F(\mathbf{d}_a, \mathbf{d}_c) = w_a f_a(\mathbf{d}_a) + w_c f_c(\mathbf{d}_a, \mathbf{d}_c)$. The vector used to quantify the coupling was derived from a comparison of the Karush-Kuhn-Tucker (KKT) optimality conditions for the coupled and uncoupled problems [12–14], and was found to be

$$\mathbf{\Gamma}_v = \frac{w_c}{w_a} \left(\frac{\partial f_c}{\partial \mathbf{d}_a} + \frac{\partial f_c}{\partial \mathbf{d}_c} \frac{d\mathbf{d}_c}{d\mathbf{d}_a} \right) \quad (4)$$

This formulation was used to study a variety of systems, including a passive/active automotive suspension [15, 16] and an elevator [17]. In addition, it has been applied to process control, particularly a spray-drying system [18]. Determination of the coupling vector requires knowledge of the system solution, since it is only meaningful at an optimal point. Strength of the coupling is determined by taking the norm of the vector, with an uncoupled system characterized by $\|\mathbf{\Gamma}_v\|_2 = 0$.

In work by Alyaqout et al. [19], bi-directional coupling was also considered. The system objective function could take any mathematical form, rather than being limited to a linear combination of the individual objectives. Any number of individual sub-systems with their own sub-system objective functions could be present, as illustrated in Fig. 1 [19]. Furthermore, the variables could have both their global values and local values, assigned to local copies of the variables, to facilitate optimization via decomposition methods [20]. The matrix used to describe coupling was derived through modifications of the Global Sensi-

tivity Equations (GSEs) to account for satisfaction of optimality conditions [21] and was found to be

$$\mathbf{\Gamma}_m = \begin{bmatrix} \frac{\partial F}{\partial f_1} \frac{\partial f_1}{\partial \mathbf{y}_{11}} \\ \vdots \\ \frac{\partial F}{\partial f_N} \frac{\partial f_N}{\partial \mathbf{y}_{1N}} \\ \vdots \\ \frac{\partial F}{\partial f_1} \frac{\partial f_1}{\partial \mathbf{y}_{N1}} \\ \vdots \\ \frac{\partial F}{\partial f_N} \frac{\partial f_N}{\partial \mathbf{y}_{NN}} \end{bmatrix}^T \begin{bmatrix} \frac{d\hat{\mathbf{y}}_{11}}{d\mathbf{x}_1} & \frac{d\hat{\mathbf{y}}_{11}}{d\mathbf{x}_2} & \dots & \frac{d\hat{\mathbf{y}}_{11}}{d\mathbf{x}_N} \\ \vdots & \vdots & \ddots & \vdots \\ \frac{d\hat{\mathbf{y}}_{1N}}{d\mathbf{x}_1} & \dots & \dots & \frac{d\hat{\mathbf{y}}_{1N}}{d\mathbf{x}_N} \\ \vdots & \vdots & \ddots & \vdots \\ \frac{d\hat{\mathbf{y}}_{N1}}{d\mathbf{x}_1} & \dots & \dots & \vdots \\ \vdots & \vdots & \ddots & \vdots \\ \frac{d\hat{\mathbf{y}}_{NN}}{d\mathbf{x}_1} & \dots & \dots & \frac{d\hat{\mathbf{y}}_{NN}}{d\mathbf{x}_N} \end{bmatrix} + \begin{bmatrix} \sum_{j=1}^N \frac{\partial F}{\partial \mathbf{x}_j} \frac{d\hat{\mathbf{x}}_j}{d\mathbf{x}_1} \\ \vdots \\ \sum_{j=1}^N \frac{\partial F}{\partial \mathbf{x}_j} \frac{d\hat{\mathbf{x}}_j}{d\mathbf{x}_N} \end{bmatrix}^T + \begin{bmatrix} \sum_{p=1}^N \sum_{j=1}^N \left(\frac{\partial F}{\partial f_p} \frac{\partial f_p}{\partial \mathbf{x}_j} \frac{d\hat{\mathbf{x}}_j}{d\mathbf{x}_1} \right) \\ \vdots \\ \sum_{p=1}^N \sum_{j=1}^N \left(\frac{\partial F}{\partial f_p} \frac{\partial f_p}{\partial \mathbf{x}_j} \frac{d\hat{\mathbf{x}}_j}{d\mathbf{x}_N} \right) \end{bmatrix}^T \quad (5)$$

This coupling measure has been used in suspension strategies in Multi-Disciplinary Optimization (MDO) [21, 22] and applied to vehicle passive/active suspension [23], electric DC motor [24], and elevator control [19]. The GSEs have been widely used in the optimization of complex coupled problems [22, 25, 26]. While this coupling measure does account for optimality conditions, as does Fathy's coupling vector, its primary origin is in the GSEs, and it appears to be far different in form from the coupling vector. Like $\mathbf{\Gamma}_v$, $\mathbf{\Gamma}_m$ is only meaningful at an optimal solution, and therefore can only be calculated once the solution is known. There are methods for the estimation of $\mathbf{\Gamma}_m$ within suspension strategies, but this requires an initial calculation of the matrix [27].

3 RELATIONSHIP BETWEEN COUPLING MEASURES

As noted previously, the coupling vector $\mathbf{\Gamma}_v$ and coupling matrix $\mathbf{\Gamma}_m$ do not have the same range of applicability. Therefore, in order to examine the relation between the two coupling measures, certain assumptions are necessary. These assumptions are:

1. The system has two objective functions, one for the artifact and one for the controller.
2. Coupling is unidirectional.
3. The overall objective function is a weighted sum of the individual objectives.
4. There are no local copies of variables.

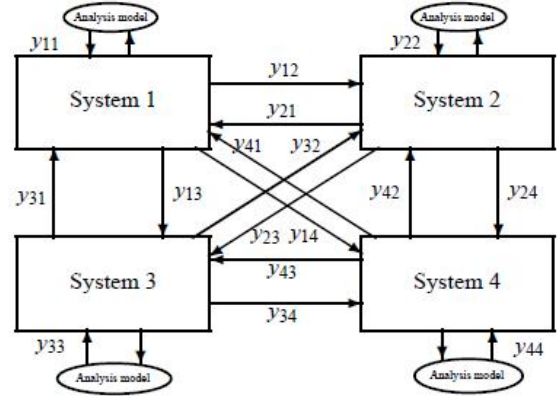


Figure 1. INTERACTION OF SUB-SYSTEMS IN GENERAL SYSTEM FORMULATION (AFTER [19])

The system in question, then, can be represented by the diagram given in Fig. 2. From assumptions 1–4, the following substitutions can be made in Eq.(5):

$$\begin{aligned} N &= 2 \\ f_1 &= f_a \\ f_2 &= f_c \\ \hat{\mathbf{x}}_1 &= \mathbf{x}_1 = \mathbf{0} \\ \hat{\mathbf{x}}_2 &= \mathbf{x}_2 = \mathbf{d}_c \\ \hat{\mathbf{y}}_{12} &= \mathbf{y}_{12} = \mathbf{d}_a \\ \hat{\mathbf{y}}_{21} &= \mathbf{y}_{21} = \mathbf{d}_a \\ \hat{\mathbf{y}}_{11} &= \mathbf{y}_{11} = \mathbf{0} \\ \hat{\mathbf{y}}_{22} &= \mathbf{y}_{22} = \mathbf{0} \end{aligned}$$

These substitutions give a simplified matrix of

$$\mathbf{\Gamma}_m = \begin{bmatrix} \mathbf{0} \\ w_a \frac{\partial f_a}{\partial \mathbf{d}_a} \frac{d\mathbf{d}_a}{d\mathbf{d}_c} + w_c \frac{\partial f_c}{\partial \mathbf{d}_a} \frac{d\mathbf{d}_a}{d\mathbf{d}_c} + w_c \frac{\partial f_c}{\partial \mathbf{d}_c} \end{bmatrix}^T \quad (6)$$

It is then possible to relate $\mathbf{\Gamma}_v$ and $\mathbf{\Gamma}_m$:

$$\mathbf{\Gamma}_m = \begin{bmatrix} \mathbf{0} \\ w_a \left(\frac{df_a}{d\mathbf{d}_c} + \left(\mathbf{\Gamma}_v - \frac{w_c}{w_a} \frac{\partial f_c}{\partial \mathbf{d}_c} \frac{d\mathbf{d}_c}{d\mathbf{d}_a} \right) \frac{d\mathbf{d}_a}{d\mathbf{d}_c} + \frac{w_c}{w_a} \frac{\partial f_c}{\partial \mathbf{d}_c} \right) \end{bmatrix}^T \quad (7)$$

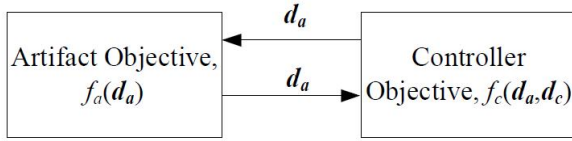


Figure 2. SUB-SYSTEM STRUCTURE FOR SIMPLIFIED SYSTEM

If it can be further assumed that the problem is also unconstrained, then Eq.(7) simplifies to

$$\mathbf{\Gamma}_m = \begin{bmatrix} 0 \\ w_a \frac{df_a}{dd_c} + w_a \mathbf{\Gamma}_v \frac{dd_a}{dd_c} \end{bmatrix}^T \quad (8)$$

The following observations can then be made:

1. $\mathbf{\Gamma}_m$ captures information about the interactions between variables in each sub-problem that is not contained within $\mathbf{\Gamma}_v$. This is consistent with the differing origins of the metrics. Since $\mathbf{\Gamma}_m$ was derived from the GSEs, it can be expected to contain information about the sensitivity of one variable to another within the same sub-system.
2. In a problem with active constraints, it is possible for $\mathbf{\Gamma}_m$ to be non-zero when $\mathbf{\Gamma}_v = \mathbf{0}$. This would indicate that relations between the design variables in a sub-system are highly significant, and the solution will be sensitive to small changes in the variables.
3. In both a constrained and an unconstrained problem, it is possible for $\mathbf{\Gamma}_m$ and $\mathbf{\Gamma}_v$ to disagree on when a system is more strongly coupled. This will happen in the case of high sensitivity in the relations between the variables.
4. For the case where constraints are active, but there is only one artifact design variable and one controller design variable, Eq.(7) simplifies to Eq.(8), just as it does for the unconstrained case. This reflects the fact that there are no possible interactions between variables within a sub-system. The same situation will occur when all active constraints consist of simple bounds.
5. If an unconstrained system is uncoupled, then $f_a = f_a(\mathbf{d}_a)$ and $f_c = f_c(\mathbf{d}_c)$. In this case, $\frac{df_a}{dd_c} = 0$ since, by definition of an uncoupled system, the artifact objective function f_a does not depend on the controller variables \mathbf{d}_c . Also, $\mathbf{\Gamma}_v = \mathbf{0}$, since the equations representing the KKT conditions will be identical for both sequential and simultaneous solutions of the system. This results in $\mathbf{\Gamma}_m = \mathbf{0}$, and therefore the two criteria will be consistent in having zero value for uncoupled problems.

4 RELATION BETWEEN COUPLING VECTOR AND PARETO FRONTIER

The combined objective in Eq.(1) implies the existence of a Pareto set. The slope of the Pareto curve (or frontier) has an interesting relationship to coupling. Note that if the Pareto frontier is non-convex, the linear scalar substitute function in Eq.(1) will need to be replaced by a nonlinear one. For the problem described here, it is possible to describe the relation between the optimum values of the two objectives as follows:

$$f_c^* = f(f_a^*) \quad (9)$$

By differentiating Eq. 9 and making appropriate substitutions, the slope of the Pareto frontier can be expressed as

$$\frac{df_c^*}{df_a^*} = \frac{w_a}{w_c} \mathbf{\Gamma}_v \frac{dd_a^*}{df_a^*} \quad (10)$$

The physical significance of the coupling vector $\mathbf{\Gamma}_v$, therefore, is that it contributes to the slope of the Pareto frontier, leading to the following observations:

1. If the coupling vector vanishes at one particular point, then the Pareto frontier will have zero slope at that point. If this point is not an end point of the Pareto frontier, then the curve will either be non-convex or discontinuous at this point.
2. It is possible for a non-zero coupling vector to be present at a point of zero slope. In this case, the coupling vector would be orthogonal to the derivative $\frac{dd_a^*}{df_a^*}$.
3. Large changes in the direction of the coupling vector, while not definitive, may be a warning sign of a non-convex or discontinuous Pareto frontier, particularly when the derivative vector $\frac{dd_a^*}{df_a^*}$ does not experience similar changes in its direction.

Information about the nature of the Pareto frontier can be useful in the design of a system. As noted, if the Pareto frontier is determined to be non-convex, then a linear combination of objectives is not an effective formulation and another formulation, such as an exponential weighted criteria function [28], will be required. If the Pareto frontier is both convex and continuous, then it can be approximated by fitting a convex continuous curve to a relatively small number of points. This can be useful when the designer wishes to find points in a particular area of the Pareto frontier. Methods do exist for finding points in specific areas of the Pareto frontier, such as the normal-boundary intersection method to find the “knee” [29]. However, the ability to approximate the curve is useful when another area of the Pareto frontier is considered to be desirable. Determination of the approximate curve has the potential to reduce the computational requirements to solve a problem.

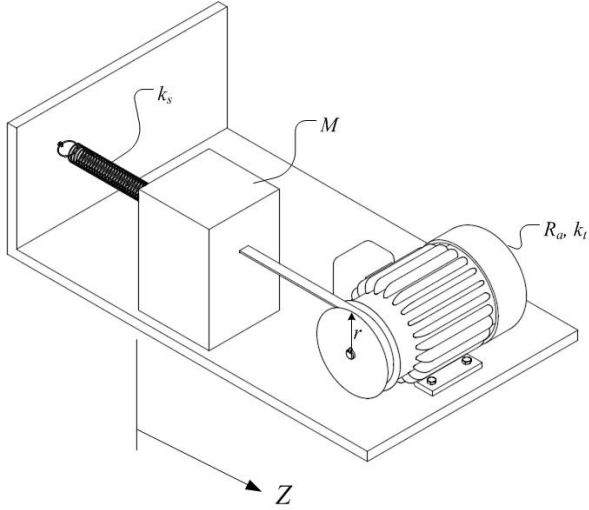


Figure 3. CONFIGURATION OF POSITIONING GANTRY

5 ILLUSTRATIVE EXAMPLE: POSITIONING GANTRY

Consider a simple model of a positioning gantry, as shown in Fig. 3. In this system, a mass M is connected to a fixed surface by a linear spring with constant k_s . A flexible inelastic belt is connected to the mass and wraps around a pulley with radius r , which is mounted on a DC motor with armature resistance R_a and motor constant k_t . The motor will be actuated by a voltage signal. The displacement of the mass from its original position is Z . The system can be modeled by the following equations:

$$\dot{\mathbf{x}} = \mathbf{A}\mathbf{x} + \mathbf{B}u \quad (11)$$

$$Z = \mathbf{C}\mathbf{x} \quad (12)$$

$$\mathbf{x} = \begin{bmatrix} Z \\ \dot{Z} \end{bmatrix} \quad (13)$$

$$\mathbf{A} = \begin{bmatrix} 0 & 1 \\ -\frac{k}{m} & -\frac{b}{m} \end{bmatrix} \quad (14)$$

$$\mathbf{B} = \begin{bmatrix} 0 \\ \frac{1}{m} \end{bmatrix} \quad (15)$$

$$\mathbf{C} = [1 \ 0] \quad (16)$$

$$u = V \quad (17)$$

$$m = \frac{MrR_a}{k_t} \quad (18)$$

$$b = \frac{k_t}{r} \quad (19)$$

$$k = \frac{k_s r R_a}{k_t} \quad (20)$$

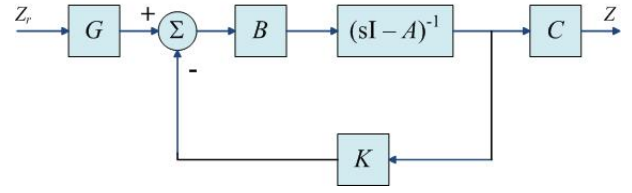


Figure 4. SCHEMATIC OF SYSTEM CONTROLLER

where the various symbols shown above are defined in the Nomenclature section of this paper.

A state-feedback controller with a precompensator G and gains $\mathbf{K} = [K_1 \ K_2]$ is applied to the system, as shown in Fig. 4. This system will be optimized twice. In both cases, constraints will be used to eliminate variables, transforming the problem into an unconstrained system that fits the description given in the preceding sections. The artifact objective function f_a will remain the same, but the artifact design variables \mathbf{d}_a and artifact constraint g_1 will be changed to produce both an uncoupled and a coupled optimization problem. The artifact objective will be to maximize the steady-state displacement of the mass, Z_{ss} . The controller objective function f_c , controller design variables \mathbf{d}_c , and controller constraint g_2 will take the same form in both formulations. The controller objective will be to minimize a combination of the maximum voltage V_{max} and the settling time t_s . The relative importance of V_{max} and t_s will be specified by parameters.

5.1 Uncoupled System Optimization

The system optimization formulation is:

$$\min_{r, k_t, K_1, K_2, G} w_a f_a + w_c f_c \quad (21)$$

subject to

$$g_1 = c_1 + \left(\frac{k_t V_{ss}}{r R_a} - c_2 \right)^{\frac{1}{2}} - r \leq 0 \quad (22)$$

$$g_2 = M_p - M_{p,all} \leq 0 \quad (23)$$

$$h_1 = Z_{ss} - Zr = 0 \quad (24)$$

The individual objectives f_a and f_c are given by

$$f_a = -Z_{ss} = -\frac{k_t V_{ss}}{r R_a k_s} \quad (25)$$

$$f_c = a_1 V_{max} + a_2 t_s \quad (26)$$

Parameter	Value
M	2.00 kg
k_s	0.75 N/mm
R_a	10.00 k Ω
V_{ss}	10.00 V
$M_{p,all}$	5%
c_1	2.50
c_2	4.00
a_1	15.00
a_2	0.25

Table 1. Parameters for Optimization of Uncoupled System

Quantity	Value	
$\mathbf{d}_a =$	r	2.50 cm
	k_t	10.00 N-m/A
$\mathbf{d}_c =$	K_1	0.72
	K_2	1.23
	G	2.59
Z_{ss}	5.33 cm	
t_s	8.79 s	
V_{max}	13.83 V	

Table 2. Results of Optimization of Uncoupled System

and the position overshoot M_p is given by

$$M_p = e^{-\pi\zeta/\sqrt{1-\zeta^2}} \quad (27)$$

$$\zeta = \frac{b + K_2}{2\sqrt{m(k + K_1)}} \quad (28)$$

where V_{ss} is the steady-state voltage applied to the motor, V_{max} is the maximum applied voltage, t_s is the 1% settling time, $M_{p,all}$ is the limit imposed on the overshoot, and Z_r is the reference signal entering the controller. The artifact weight w_a and the controller weight w_c have strictly positive values between 0 and 1. The constraint g_1 is formulated to ensure that the pulley radius r is appropriate for the thickness of belt required for the forces present.

The constraints were determined to be active by monotonicity analysis and were used to eliminate the variables k_t , G , and

K_1 , which creates a problem in which Eq. (8) is applicable. Using the values shown in Table 1, the optimum solution and both coupling metrics were calculated. The optimal values of the design variables and of Z_{ss} , V_{max} , and t_s are given in Table 2. For all values of w_a and w_c in the specified range, $\Gamma_v = 0$ and $\mathbf{\Gamma}_m = [0 \ 0]$, and therefore both measures were consistent in indicating that the system is uncoupled. These coupling measures are also consistent with the results of the system optimization itself; identical results were found for both sequential optimization and for simultaneous optimization with various combinations of weights.

5.2 Coupled System Optimization

Now, consider a different formulation of the system optimization. In this case, the design variables are k_s , R_a , G , K_1 , and K_2 , the objective functions and constraints g_2 and h_1 are unchanged, but constraint g_1 is changed. The new constraint g_1 is formulated to ensure that the spring is sized appropriately for the loads present.

$$\min_{k_s, R_a, K_1, K_2, G} w_a f_a + w_c f_c \quad (29)$$

subject to

$$g_1 = \left(\frac{V_{ss} k_t}{r R_a} + c_4 \right)^{1.5} - c_3 - k_s \leq 0 \quad (30)$$

$$g_2 = M_p - M_{p,all} \leq 0 \quad (31)$$

$$h_1 = Z_{ss} - Z_r = 0 \quad (32)$$

where f_a and f_c are given by Eq.(25) and (26), respectively.

Again, monotonicity analysis was used to determine that all constraints were active, and they were used to eliminate the variables k_s , G , and K_1 , producing an unconstrained system. Again, this creates a problem in which Eq. (8) is applicable. The problem was solved for the parameters in Table 3 and several sets of weights. Results for two sets of weights are given in Table 4. The first set given corresponds to the point ‘‘A’’ and the second set of weights to the point ‘‘B’’ in Fig. 5.

In this case, both coupling measures are non-zero. This agrees with the results of the system optimization; assigning different weights to the objectives f_a and f_c in the simultaneous system solution yields different results. The sequential problem cannot be solved in this case without additional constraints, since it is unbounded. It can also be noted that the calculated slope of the Pareto frontier given in Table 4 appears reasonable; estimation of the slope from the points shown in Fig. 5 agrees with the calculated results.

At no point does Γ_v vanish, nor does it experience any sign changes. While this is a necessary condition for a convex contin-

Parameter	Value
M	2.00 kg
k_t	10.00 N-m/A
r	2.50 cm
V_{ss}	10.00 V
$M_{p,all}$	5%
c_3	1.50
c_4	1.00
a_1	15.00
a_2	0.20

Table 3. Parameters for Optimization of Coupled System

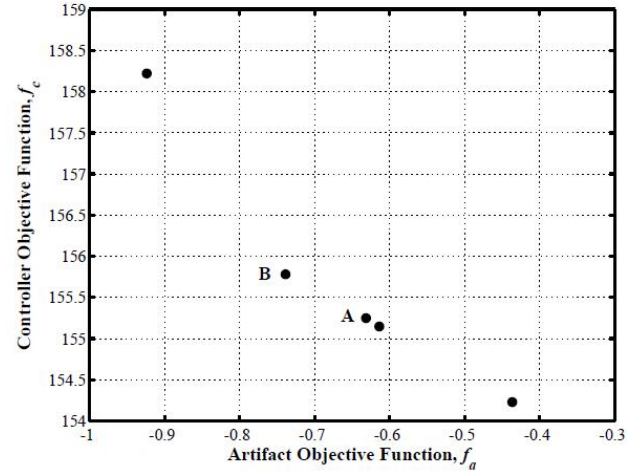


Figure 5. PARETO FRONTIER FOR COUPLED SYSTEM OPTIMIZATION

Therefore, it is conjectured that the Pareto frontier will be convex and continuous, and that it would be possible to estimate the full Pareto frontier by fitting a continuous convex curve to the points shown.

6 RELATION BETWEEN COUPLING VECTOR AND EASE OF CONTROL SURROGATE FUNCTION

If the coupling vector for a design and control optimization problem vanishes, then the system optimum can be found by a sequential optimization of the artifact and controller. This is not the case for a system with a non-zero coupling vector. However, since sequential optimization offers the advantages of lower computational demands, the separation of the problem by discipline, and the ability to apply techniques such as optimal control theory, it is the preferred method of solving the co-design problem. Therefore, a modified sequential approach (Fig. 6) that would produce the solution set of the original problem is desirable. This raises the question of what form such a modified sequential problem might take, and how it relates to the coupling.

Assume that some surrogate for ease of control $\chi(\mathbf{d}_a)$ is introduced into the artifact objective function, such that the modified artifact objective is given by $f'_a(\mathbf{d}_a) = w_1 f_a(\mathbf{d}_a) + w_2 \chi(\mathbf{d}_a)$. The weights w_1 and w_2 can be varied to produce a set of designs, for which the controller objective function can then be optimized. The modified problem, then, can be formulated as

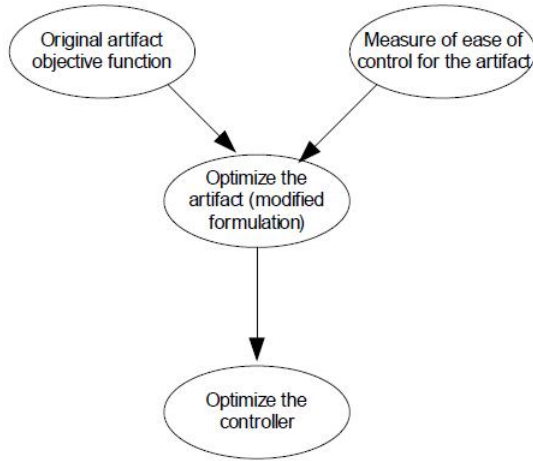
$$\min_{\mathbf{d}_a} f'_a(\mathbf{d}_a) = w_1 f_a(\mathbf{d}_a) + w_2 \chi(\mathbf{d}_a) \quad (33)$$

$$\min_{\mathbf{d}_c} f_c(\arg \min_{\mathbf{d}_a} f'_a(\mathbf{d}_a), \mathbf{d}_c) \quad (34)$$

Quantity	Value for Given Weights	
	$w_a = 0.4, w_c = 0.6$	$w_a = 0.7, w_c = 0.3$
$\mathbf{d}_a = \begin{matrix} R_a \\ k_s \end{matrix}$	$\begin{matrix} 28.60 \text{ k}\Omega \\ 2.21 \text{ N/mm} \end{matrix}$	$\begin{matrix} 38.75 \text{ k}\Omega \\ 1.40 \text{ N/mm} \end{matrix}$
$\mathbf{d}_c = \begin{matrix} K_1 \\ K_2 \\ G \end{matrix}$	$\begin{matrix} -1.43 \\ 15.81 \\ 14.40 \end{matrix}$	$\begin{matrix} -2.15 \\ 16.50 \\ 11.38 \end{matrix}$
Z_{ss}	0.63 cm	0.74 cm
t_s	6.64 s	8.70 s
V_{max}	10.26 V	10.27 V
Γ_v	0.058	0.113
Γ_m	$\begin{bmatrix} 0 \\ 0.0039 \end{bmatrix}^T$	$\begin{bmatrix} 0 \\ -0.0033 \end{bmatrix}^T$
Calculated Slope of the Pareto Frontier Using Eq. (10)	-3.73	-23.86

Table 4. Results of Optimization of Coupled System

uous Pareto frontier, it is not sufficient in the general case. However, in the unconstrained problem solved here, there is only one independent artifact design variable d_a . In this case, the Pareto frontier will be convex and continuous as long as the derivative $\frac{d\mathbf{d}_a^*}{df_a}$ does not vanish at any point. Neither this derivative, nor the coupling vector, vanishes for any of the points computed.



Sequential Design for Ease of Control

Figure 6. MODIFIED SEQUENTIAL SOLUTION METHOD

subject to

$$\mathbf{g}_a(\mathbf{d}_a) \leq \mathbf{0} \quad (35)$$

$$\mathbf{h}_a(\mathbf{d}_a) = \mathbf{0} \quad (36)$$

$$\mathbf{g}_c(\arg \min f'_a(\mathbf{d}_a), \mathbf{d}_c) \leq \mathbf{0} \quad (37)$$

$$\mathbf{h}_c(\arg \min f'_a(\mathbf{d}_a), \mathbf{d}_c) = \mathbf{0} \quad (38)$$

The KKT conditions for this system can be written as

$$\begin{bmatrix} \frac{\partial f_a}{\partial \mathbf{d}_a} + \frac{\partial \chi}{\partial \mathbf{d}_a} \\ \frac{\partial f_c}{\partial \mathbf{d}_c} \end{bmatrix} + \boldsymbol{\lambda}^T \begin{bmatrix} \frac{\partial \mathbf{h}_a}{\partial \mathbf{d}_a} \\ \frac{\partial \mathbf{h}_c}{\partial \mathbf{d}_c} \end{bmatrix} + \boldsymbol{\mu}^T \begin{bmatrix} \frac{\partial \mathbf{g}_a}{\partial \mathbf{d}_a} \\ \frac{\partial \mathbf{g}_c}{\partial \mathbf{d}_c} \end{bmatrix} = \mathbf{0} \quad (39)$$

$$\boldsymbol{\mu}^T \begin{bmatrix} \mathbf{g}_a \\ \mathbf{g}_c \end{bmatrix} = \mathbf{0} \quad (40)$$

$$\boldsymbol{\lambda} \neq \mathbf{0} \quad (41)$$

$$\boldsymbol{\mu} \geq \mathbf{0} \quad (42)$$

Assume that the surrogate term is chosen such that, for any sets of weights w_a and w_c in the original problem, there exists some set of strictly positive weights w_1 and w_2 that will generate the identical solution from the modified problem. In this case, the KKT conditions can be equated, leading to the following relation:

$$\frac{w_2}{w_1} \frac{\partial \chi}{\partial \mathbf{d}_a} = \boldsymbol{\Gamma}_v \quad (43)$$

It can be observed from Eq. (43) that such a set of weights will exist, and the modified sequential problem will produce the Pareto optimal solutions, when the gradient of the surrogate $\nabla \chi$ is parallel to the coupling vector $\boldsymbol{\Gamma}_v$. This relation could be used to evaluate the suitability of a particular surrogate function to determine its accuracy in approximating the original problem. The angle between the two vectors $\nabla \chi$ and $\boldsymbol{\Gamma}_v$ could be evaluated, with a small angle corresponding to a close solution. A large angle between the two vectors would indicate a poor choice of surrogate function. If an appropriate surrogate function can be found for a given type of problem, then it would be unnecessary to calculate $\boldsymbol{\Gamma}_v$, and that type of problem could be solved sequentially. Such modified sequential formulations have been shown highly effective in some cases [9]. Furthermore, it indicates that in the case where there is only one artifact design variable \mathbf{d}_a , any surrogate function with appropriate monotonicity will be effective. Note, however, that the distribution of points for a given set of weights will differ in the original and modified problem.

7 EXTENSION OF COUPLING VECTOR TO BI-DIRECTIONAL COUPLING

As previously stated, the coupling vector $\boldsymbol{\Gamma}_v$ was derived based on the assumption of uni-directional coupling. While there are many systems which exhibit uni-directional coupling, bi-directional coupling is also an important phenomenon. Therefore, it is useful to extend the coupling vector to these cases. The extended coupling vector $\boldsymbol{\Gamma}_{vb}$ can be found through the same procedure used to derive the coupling vector $\boldsymbol{\Gamma}_v$ [14]. Given the system

$$\min_{\mathbf{d}_a, \mathbf{d}_c} f = w_a f_a(\mathbf{d}_a, \mathbf{d}_c) + w_c f_c(\mathbf{d}_a, \mathbf{d}_c) \quad (44)$$

subject to

$$\mathbf{g}(\mathbf{d}_a, \mathbf{d}_c) \leq \mathbf{0} \quad (45)$$

$$\mathbf{h}(\mathbf{d}_a, \mathbf{d}_c) = \mathbf{0} \quad (46)$$

its solution must satisfy the KKT stationarity condition

$$\nabla f_* + \boldsymbol{\lambda}^T \nabla \mathbf{h}_* + \boldsymbol{\mu}^T \nabla \mathbf{g}_* = \mathbf{0}^T \quad (47)$$

Using the difference between the KKT stationarity conditions for the sequential and simultaneous solutions, the coupling vector for the case of bi-directional coupling is found to be

$$\boldsymbol{\Gamma}_{vb} = \begin{bmatrix} \frac{w_c}{w_a} \left(\frac{\partial f_c}{\partial \mathbf{d}_a} + \frac{\partial f_c}{\partial \mathbf{d}_c} \frac{d\mathbf{d}_c}{d\mathbf{d}_a} \right) \frac{\partial f_a}{\partial \mathbf{d}_c} + \frac{\partial f_a}{\partial \mathbf{d}_a} \frac{d\mathbf{d}_a}{d\mathbf{d}_c} \end{bmatrix} \quad (48)$$

Note that the uni-directional coupling vector appears within the extended coupling vector, and Eq. (48) can be re-written as

$$\mathbf{\Gamma}_{vb} = \left[\mathbf{\Gamma}_v \frac{\partial f_a}{\partial \mathbf{d}_c} + \frac{\partial f_a}{\partial \mathbf{d}_a} \frac{d\mathbf{d}_a}{d\mathbf{d}_c} \right] \quad (49)$$

As with the uni-directional coupling vector $\mathbf{\Gamma}_v$, the strength of the coupling present can be quantified by evaluating the vector norm $\|\mathbf{\Gamma}_{vb}\|_2$. As in the case of $\mathbf{\Gamma}_v$, $\mathbf{\Gamma}_{vb}$ captures information about the interactions between sub-systems, but does not provide any insight into the relationships between variables within a sub-system, as does $\mathbf{\Gamma}_m$. The relationship between $\mathbf{\Gamma}_{vb}$ and $\mathbf{\Gamma}_m$ merits further investigation.

8 CONCLUDING REMARKS

The existence of coupling in a system can be demonstrated by using either the coupling vector or the coupling matrix. The results will be consistent, despite the differing origins and theoretical basis of the two coupling measures. This raises the question of when each measure is most appropriate.

In the cases where $\mathbf{\Gamma}_v$ applies, it is easier to calculate, has a clear physical interpretation, and would be the preferred method of evaluating coupling. On the other hand, there are circumstances in which $\mathbf{\Gamma}_v$ does not apply. If coupling is bi-directional, multiple sub-systems exist, or the overall objective function cannot be expressed as a linear combination of the individual functions, then $\mathbf{\Gamma}_v$ cannot be used, and $\mathbf{\Gamma}_m$ would be the preferred metric. Furthermore, $\mathbf{\Gamma}_m$ would be useful in cases where a solution strategy based on decomposition and coordination is to be used, since it explicitly accounts for local and global copies of variables, and can be used in suspension strategies. In some cases of uni-directional coupling where constraints cannot be easily eliminated, it may be difficult to determine which metric is most useful. Although $\mathbf{\Gamma}_v$ is applicable in these cases, it fails to capture all information about the interactions between the variables.

$\mathbf{\Gamma}_v$ was shown to have an interpretation as a component of the slope of the Pareto frontier. This indicates that changes in the coupling vector can provide insight into the nature of the Pareto frontier of the system, including the existence of discontinuities and non-convexity. If the coupling vector at a small number of points is known, it can be used to estimate the behavior of the Pareto frontier between those points. This can assist a designer in choosing which locations on the Pareto frontier are most appropriate in his or her specific problem, and effort can be devoted to computing solutions in that region of the Pareto frontier. This would decrease the overall computational effort required to solve the problem, without any loss of accuracy in the solution.

$\mathbf{\Gamma}_v$ was further shown to provide a means to determine whether a given surrogate for ease of control can be used to formulate a modified sequential problem. If the gradient of a can-

didate surrogate function χ is parallel to $\mathbf{\Gamma}_v$, then it will provide the exact solution set.

Finally, the coupling vector can be extended to provide a measure of bi-directional coupling. This can be used, as can the uni-directional coupling vector, as a measure of coupling strength. It is anticipated that it will also have a variety of physical interpretations similar to those for the uni-directional case.

Future work should explore the use of a surrogate function for ease of control in a modified sequential formulation. In addition, future work should evaluate the estimation of coupling a priori, in order to use that information in selection of appropriate solution methods for the combined design and control problem.

ACKNOWLEDGMENT

This work was partially supported by NSF grant #0625060. This support is gratefully acknowledged.

REFERENCES

- [1] Belvin, W., and Park, K. "Structural tailoring and feedback control synthesis: an interdisciplinary approach". *AIAA Journal*.
- [2] Haftka, R. "Integrated structure/control optimization of space structures". *AIAA Journal*.
- [3] Milman, M., Salama, M., Scheid, R., Bruno, R., and Gibson, J., 1991. "Combined control-structural optimization". *Computational Mechanics*, **8**(1), January, pp. 1–18.
- [4] Ravichandran, T., Wang, D., and Heppler, G., 2006. "Simultaneous plant-controller design optimization of a two-link planar manipulator". *Mechatronics*, **16**(1), January, pp. 233–242.
- [5] Zhang, W., Li, Q., and Guo, L., 1999. "Integrated design of mechanical structure and control algorithm for a programmable four-bar linkage". *IEEE/ASME Transactions on Mechatronics*, **4**(4), December, pp. 354–362.
- [6] Zhu, Y., Qiu, J., and Tani, J., 2001. "Simultaneous optimization of a two-link flexible robot arm". *Journal of Robotic Systems*, **18**(1), January, pp. 29–38.
- [7] Carley, L., Ganger, G., Guillou, D., and Nagle, D., 2001. "System design considerations for mems-actuated magnetic-probe-based mass storage". *IEEE Transactions on Magnetics*, **37**(2), March, pp. 657–662.
- [8] Wolfram, H., Schmiedel, R., Hiller, K., Aurich, T., Gunther, W., Kurth, S., Mehner, J., Dotzel, W., and Gebner, T., 2005. "Model building, control design and practical implementation of a high precision, high dynamical mems acceleration sensor". In Proceedings of SPIE, Volume 5836: Smart Sensors, Actuators, and MEMS II, C. Cane, J. Chiao, and F. V. Verdu, eds., SPIE.
- [9] Peters, D. L., Kurabayashi, K., Papalambros, P. Y., and Ulsoy, A. G., 2008. "Co-design of a mems actuator and

- its controller using frequency constraints”. In Proceedings of the ASME Dynamic Systems and Control Conferences, ASME. Paper number DSCC2008-2212.
- [10] Reyer, J. A., and Papalambros, P. Y., 2002. “Combined optimal design and control with application to an electric dc motor”. *Journal of Mechanical Design*, **124**(2), June, pp. 183–191.
- [11] Reyer, J. A., and Papalambros, P. Y., 2000. “An investigation into modeling and solution strategies for optimal design and control”. In Proceedings of the ASME Design Engineering Technical Conferences, J. M. Vance, ed., Vol. **2**, ASME, pp. 283–292. Paper number DETC 2000/DAC-14253.
- [12] Fathy, H., Papalambros, P. Y., and Ulsoy, A. G., 2004. “On combined plant and control optimization”. In 8th Cairo University International Conference on Mechanical Design and Production.
- [13] Reyer, J. A., Fathy, H., Papalambros, P. Y., and Ulsoy, A. G., 2001. “Comparison of combined embodiment design and control optimization strategies using optimality conditions”. In Proceedings of the ASME Design Engineering Technical Conferences, J. E. Renaud, ed., Vol. **2**, ASME, pp. 1023–1032. Paper number DETC 2001/DAC-21119.
- [14] Fathy, H., Reyer, J. A., Papalambros, P. Y., and Ulsoy, A. G., 2001. “On the coupling between the plant and controller optimization problems”. In IEEE American Control Conference, B. H. Krogh, ed., Vol. **3**, IEEE, pp. 1864–1869.
- [15] Fathy, H., Papalambros, P. Y., and Ulsoy, A. G., 2003. “Integrated plant, observer, and controller optimization with application to combined passive/active automotive suspensions”. In Proceedings of the 2003 ASME Mechanical Engineering Congress and Exposition, ASME. IMECE2003-42014.
- [16] Fathy, H., Papalambros, P. Y., Ulsoy, A. G., and Hrovat, D., 2003. “Nested plant/controller optimization with application to combined passive/active automotive suspensions”. In IEEE American Control Conference, B. W. Bequette, ed., Vol. **4**, ASME, pp. 3375–3380.
- [17] Fathy, H., Bortoff, S. A., Papalambros, P. Y., Ulsoy, A. G., and Copeland, S. G., 2002. “Nested optimization of an elevator and its gain-scheduled lqg controller”. In Proceedings of the 2003 ASME Mechanical Engineering Congress and Exposition, ASME. IMECE2002-34273.
- [18] Shabde, V. S., and Hoo, K. A., 2008. “Optimum controller design for a spray drying process”. *Control Engineering Practice*, **16**(5), May, pp. 541–552.
- [19] Alyaqout, S. F., Papalambros, P. Y., and Ulsoy, A. G., 2005. “Quantification and use of system coupling in decomposed design optimization”. In Proceedings of the 2005 ASME Mechanical Engineering Congress and Exposition, ASME. IMECE2005-81364.
- [20] Allison, J., Kokkolaras, M., and Papalambros, P. Y., 2005. “On the impact of coupling strength on complex system optimization for single-level formulations”. In International Design Engineering Technical Conferences & Computers and Information in Engineering Conference, ASME. DETC2005-84790.
- [21] Alyaqout, S. F., Papalambros, P. Y., and Ulsoy, A. G., 2007. “Coupling in design and robust control optimization”. In European Control Conference.
- [22] English, K., Bloebaum, C. L., and Miller, E., 2001. “Development of multiple cycle coupling suspension in the optimization of complex systems”. *Structural and Multidisciplinary Optimization*, **22**(4), November, pp. 268–283.
- [23] Alyaqout, S. F., Papalambros, P. Y., and Ulsoy, A. G., 2007. “Combined design and robust control of a vehicle passive/active suspension”. In European Control Conference.
- [24] Alyaqout, S. F., Papalambros, P. Y., and Ulsoy, A. G., 2006. “Combined robust design and robust control of an electric dc motor”. In Proceedings of the 2006 ASME Mechanical Engineering Congress and Exposition, ASME. IMECE2006.
- [25] Sobieszczanski-Sobieski, J. “On the sensitivity of complex, internally coupled systems”. *AIAA Journal*, **28**.
- [26] Bloebaum, C. L., and Hajela, P., 1991. “Heuristic decomposition for non-hierarchic systems”. In Proceedings of AIAA/ASME/ASCE/AHS 32nd Structures, Structural Dynamics, and Materials Conference, AIAA. AIAA-91-1039.
- [27] Alyaqout, S., 2006. “A Multi-System Optimization Approach to Coupling in Robust Design and Control”. PhD Thesis, University of Michigan, Ann Arbor, MI, April.
- [28] Athan, T., 1994. “A Quasi-Monte Carlo Method for Multicriteria Optimization”. PhD Thesis, University of Michigan, Ann Arbor, MI, April.
- [29] Das, I., 1999. “On characterizing the “knee” of the pareto curve based on normal-boundary intersection”. *Structural and Multidisciplinary Optimization*, **18**(2), October, pp. 107–115.